

IR absorption spectrum of CrO_2Cl_2 molecules prepared in a high-lying state of a vibrational quasicontinuum

A. V. Evseev, V. M. Krivtsov, Yu. A. Kuritsyn, A. A. Makarov, A. A. Pureskiĭ,
E. A. Ryabov, E. P. Snegirev, and V. V. Tyakht

Spectroscopy Institute, USSR Academy of Sciences

(Submitted 3 January 1984)

Zh. Eksp. Teor. Fiz. **87**, 111–124 (July 1984)

A new method for spectroscopy of highly excited vibrational states of polyatomic molecules is realized. CrO_2Cl_2 molecules were prepared in states with approximate vibrational energy 19000 cm^{-1} in the ground electronic state A_1 by internal conversion of the electron energy from the electron-excited state B_1 pumped by laser radiation. The spectroscopy of the vibrationally excited molecules was implemented in the region of the bands ν_0 and ν_1 with the aid of a diode laser and a CO_2 laser. A spectrum with approximate width of about 15 cm^{-1} at half-maximum was obtained. A theoretical analysis is given of the intermode-interaction mechanism in the CrO_2Cl_2 molecule, and the calculated spectrum is compared with the measured one. The evolution of the spectrum of the vibrationally excited CrO_2Cl_2 molecules in time is studied. It is shown that the average energy transferred in one collision with an unexcited CrO_2Cl_2 molecule is $\langle \Delta E \rangle \approx 1200\text{ cm}^{-1}$.

INTRODUCTION

Processes connected with strong vibrational activation of polyatomic molecules are being intensively studied of late.¹ For the understanding of these processes, great interest attaches to the spectroscopy of vibrationally excited molecules. A distinguishing feature of vibrationally excited molecules is homogeneous broadening of individual spectral lines, due to mixing of close-lying vibrational state through intermode anharmonicity. This mixing produces a vibrational quasicontinuum (QC) of the molecule.

Only few experiments on direct probing of the QC have been reported so far. In most cases the theoretical interpretation of such experiments is made difficult by the inhomogeneous broadening due to the molecule distribution over the vibrational states. This broadening is inherent, for example, in the usual method of reading molecules in QC states in the course of multiphoton IR excitation.¹ To carry out spectroscopy in the QC it is necessary to eliminate as much as possible the investigated-spectrum broadening due to the distribution of the molecules over the vibrational states. It is therefore better to use for spectroscopy of high vibrational states methods that permit probing of the monoenergetic QC states. Such methods include, in particular, direct spectroscopy of the high overtones and reading of the molecules in the high vibrational states via nonradiative transitions in the course of intramolecular conversion.

A number of papers on the spectroscopy of high overtones of polyatomic molecules are known at present.^{2–5} Thus, for example, narrow vibrational-rotational lines of Doppler width have been observed² in the acetylene molecule for the fifth and sixth overtones of the C–H vibration, i.e., for vibrational energies $14900\text{--}18500\text{ cm}^{-1}$. In the molecules SiHCl_3 and SiH_2Cl_2 , no noticeable broadening of the vibrational-rotational contour was observed when the number of Si–H vibration overtones was increased from $\Delta\nu = 6$ to $\Delta\nu = 9$, corresponding to vibrational energies 12000--

18000 cm^{-1} (Ref. 3). As the molecules become more complex, the picture changes. Bands $50\text{--}100\text{ cm}^{-1}$ wide, depending on the number of the excited C–H vibration overtone, are observed for the benzene molecule.⁴ For the more complicated tetramethyl-dioxetane, the width of the fifth overtone of the C–H mode is 100 cm^{-1} (Ref. 5).

The purpose of the present paper is the study of the IR absorption of CrO_2Cl_2 molecules readied quasimonenergetically into states with approximate vibrational energy 19000 cm^{-1} , which is only 4000 cm^{-1} lower than its dissociation limit. The molecules were readied in the high vibrational states in the course of intramolecular conversion of the electronic energy into vibrational by molecular absorption of visible laser radiation. As a result, a relatively narrow IR absorption band was observed, corresponding to transitions from a state with approximate energy 19000 cm^{-1} . The observed spectrum is theoretically interpreted. The time evolution of this absorption band is also studied.

1. SPECTRAL CHARACTERISTICS OF CrO_2Cl_2 MOLECULE

The lower electron-vibrational states of the CrO_2Cl_2 molecule were sufficiently well investigated.^{6,7} A critical review of the available experimental results is given in Ref. 7. Located below the dissociation level of the electronic ground state 1A_1 are two singlet states A_2 and B_1 with 0–0 transition energies 16970 and 17248 cm^{-1} , respectively. The density of the vibrational levels of the electronic ground state near the energy 17248 cm^{-1} is $6.5 \cdot 10^6\text{ 1/cm}^{-1}$. Owing to the nonadiabatic interaction of the ground A_1 and the electron-excited B_1 electronic states, the B_1 vibrational levels undergo nonradiative transitions. These transitions were revealed in experiment by the shortening of the time of fluorescent decay with increasing frequency of the pump radiation.⁶ No fluorescence was observed in pumping of states with energy more than 450 cm^{-1} higher than the 0–0 transition energy. In our experiment the CrO_2Cl_2 molecules were excited by

TABLE I. Frequency of normal vibrations of the CrO_2Cl_2 molecule.^{7,8}

Symmetry	Mode	(cm^{-1})	Type of vibration	
$A_1(z)$	{	ν_1	995 *	valence
		ν_2	475 *	valence
		ν_3	356 *	deformation
		ν_4	140 **	deformation
A_2	{	ν_5	224 **	torsion
$B_1(x)$	{	ν_6	1002 *	valence
		ν_7	215 **	pendulum
$B_2(y)$	{	ν_8	500 *	valence
		ν_9	257 **	pendulum

*Data obtained in gas⁹;

**data obtained in liquid^{10,11}

the second harmonic of the Nd:YAG laser; the frequency of this harmonic was 1550 cm^{-1} higher than the energy of the 0-0 transition. The cross section for absorption at the pump wavelength ($\lambda = 532 \text{ nm}$) is $3.8 \cdot 10^{-19} \text{ cm}^2$. At such energy levels, the molecules are in an isoenergetic vibrational state of the ground electronic term as a result of the nonradiative transition. The quasienergetic molecule ensemble readied in this manner was further probed with IR radiation.

Table I lists the vibrational frequencies of the CrO_2Cl_2 molecule.^{7,8} The rotational constants of this molecules (in cm^{-1}) are $A = 0.1073$, $B = 0.0620$, and $C = 0.0521$ (Ref. 7). A characteristic feature of this molecule is the presence of a large number of low-frequency vibrations. There are only two high-frequency modes, ν_1 and ν_6 , both active in the IR absorption spectrum. The CrO_2Cl_2 molecules were probed with IR laser radiation in the region of the bands ν_1 and ν_6 .

2. EXPERIMENT

The absorption spectrum of vibrationally high-excited CrO_2Cl_2 molecules was investigated with the setup shown in Fig. 1. The molecules were excited by the second harmonic of a 532-nm Nd:YAG laser. The maximum second-harmonic energy of this laser was 20 mJ, the pulse duration 15 nsec, the radiation spectral width 15 nsec, and the diameter of the

exciting beam in the cell 8 mm.

The excited molecules were probed with the IR lasers used to measure the induced-absorption spectrum. To cover as wide an induced-radiation spectral band as possible, three IR laser types were used: a diode laser based on PbSnSe crystal covered the $950\text{--}1020 \text{ cm}^{-1}$ band, and $^{12}\text{CO}_2$ and $^{13}\text{CO}_2$ lasers operated in the $800\text{--}900 \text{ cm}^{-1}$ band. The probing radiation power did not exceed several milliwatt for the CO_2 laser and amounted to several hundred microwatt for the diode laser. The Nd:YAG and the diode lasers were synchronized within not less than 30 nsec.

The exciting and probing beams were guided into a glass cell 50 cm long with NaCl windows. The IR radiation passing through the cell was focused onto a monochromator slit. The monochromator served for frequency tie-in of the probing radiation and acted as a filter that cut off the parasitic background light.

The IR radiation passing through the monochromator was recorded with an IR receiver based on an Si:B crystal operating at liquid-helium temperature. The receiver sensitivity threshold was $10^{-11} \text{ W Hz}^{-1/2}$, and its dynamic range was 10^7 . The time resolution was 150 nsec. The recording system could detect a 0.1% change of the absorption coefficient at a signal/noise ratio equal to 3.

We measured in the experiment absorption (clearing) induced by the second harmonic of the Nd:YAG laser and characterized by an induced-absorption (clearing) coefficient $k_{\text{ind}}(t)$. The change of the probing-radiation intensity is defined as

$$\Delta I(t) = I_0 \exp(-kL) [1 - \exp(-k_{\text{ind}}(t)L)], \quad (1)$$

where I_0 is the incident-radiation intensity, k is the linear-absorption coefficient, and L is the cell length. In the case $k_{\text{ind}} \ll 1$ we have

$$k_{\text{ind}}(t) \approx \Delta I(t) / LI_0 e^{-kL} = \Delta I(t) / LI, \quad (2)$$

where I is the intensity of the probing radiation passing through the cell in the absence of the pump radiation.

3. RESULTS OF EXPERIMENT

Figure 2 shows typical oscillograms of the induced absorption and clearing $k_{\text{ind}}(t)$ obtained by proving CrO_2Cl_2 molecules in different regions of the IR spectrum near the bands ν_1 and ν_6 . Probing at the frequency 930 cm^{-1} produced an induced absorption signal with a steep leading

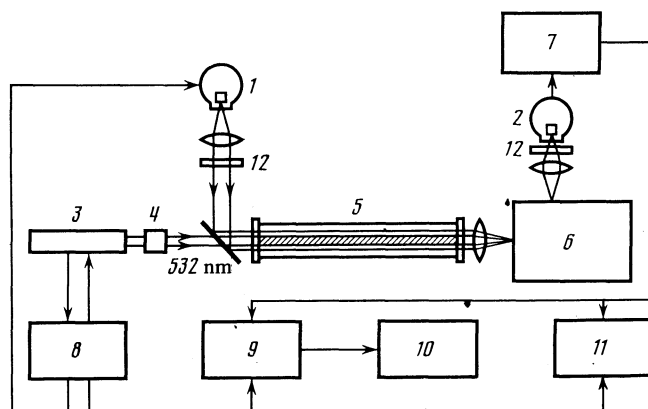


FIG. 1. Diagram of experimental setup. 1—IR lasers ($^{12}\text{CO}_2$, $^{13}\text{CO}_2$, diode laser based on PbSnSe crystal); 2—IR receiver based on Si:B crystal; 3—Nd:YAG laser; 4—CDA crystal; 5—gas cell; 6—monochromator; 7—U3-29 amplifier; 8—synchronization block; 9—data gathering and processing system; 10—automatic plotter; 11—S8-12 oscilloscope; 12—germanium plate.

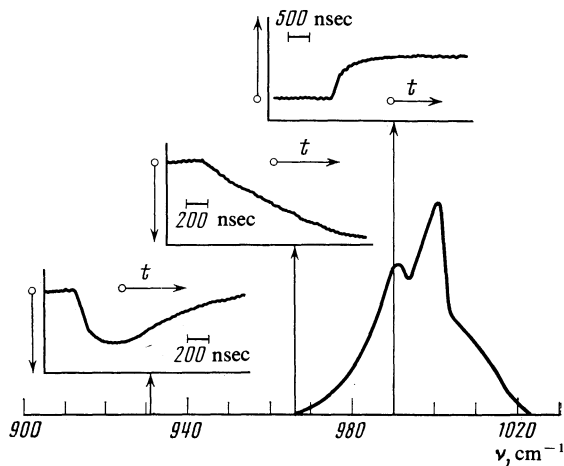


FIG. 2. Oscillogram of induced absorption (downward arrow) and bleaching (upward arrow) pulses obtained by probing at the frequencies 931.0, 966.2, and 989.6 cm^{-1} . Also shown is the CrO_2Cl_2 IR absorption spectrum corresponding to the modes ν_1 and ν_6 . The oscillograms were obtained at a CrO_2Cl_2 gas pressure 0.5 Torr in the cell.

front. The rise time remained unchanged when the CrO_2Cl_2 gas pressure was varied in the range 0.05–0.5 Torr. The maximum amplitude of this signal varies linearly with the gas pressure in the cell. The absorption induced at 930 cm^{-1} is therefore collisionless and is due to monomolecular processes that occur when the CrO_2Cl_2 molecule is pumped. The induced-absorption amplitude at 930.0 cm^{-1} varies linearly both with the pump energy in the range 0–20 mJ/cm^2 , and with the probing radiation power 0–5 mW.

As the absorption bands ν_1 and ν_6 of the unexcited molecules are approached the induced-absorption pulse waveform changes substantially. The leading front of the pulse becomes longer, meaning that collisional induced absorption appears in this frequency region. Probing in the bands ν_1 and ν_6 themselves produces a clearing signal corresponding to depletion of a number of lower vibrational-rotational levels of the CrO_2Cl_2 molecule. The duration of the leading front of the clearing pulse is also determined by the time constant of the recording system.

Figure 3 shows the induced-absorption spectra obtained at different instants of time after the pump pulse. These spectra were obtained from the induced-absorption pulses (Fig. 2) taken at the instants 0.1, 0.25, 0.5, and 1 μsec at the corresponding frequencies. The induced-absorption spectrum obtained at 0.1 μsec after the pump pulse is a rather narrow band of width 15 cm^{-1} (at half maximum). On the blue side of this band is observed a relatively low-intensity base. At $\approx 980\text{ cm}^{-1}$ the amplitude of this base decreases because of the induced clearing of the fundamental absorption band. In the succeeding instants of time and intensity $k_{\text{ind}}(\omega, t)$ of the induced absorption decreases, the band broadens, and its maximum shifts towards the fundamental bands ν_1 and ν_6 . Collisional absorption appears simultaneously on the red wing of the ν_1 and ν_6 bands.

We note that the induced absorption band $k_{\text{ind}}(\omega, t = 0.1\text{ }\mu\text{sec})$ is somewhat narrower than the inhomogeneously broadened absorption bands ν_1 and ν_6 of the CrO_2Cl_2 at $T = 300\text{ K}$. At room temperature, owing to the presence

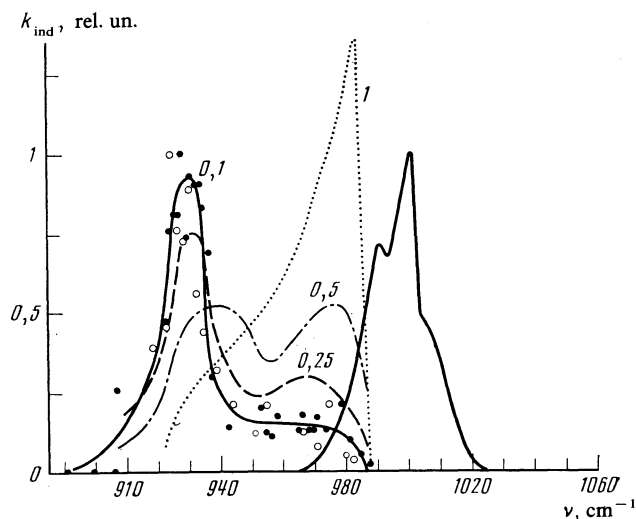


FIG. 3. Induced-absorption spectra obtained at the instants 0.1, 0.25, 0.5 and 1 μsec after the pump pulse. The points pertain to the induced-absorption spectrum shown by the solid curve for the time 0.1 μsec . The dark and light circles pertain to probing by $^{13}\text{CO}_2$ and $^{12}\text{CO}_2$ lasers, respectively. The exciting-radiation density is 20 mJ/cm^2 , the gas pressure in the cell is 0.5 Torr. On the right is shown for comparison the spectrum of the linear IR absorption of the CrO_2Cl_2 molecule, corresponding to the modes ν_1 and ν_6 . The amplitude of this spectrum is not drawn to the same scale as the amplitude of the induced-absorption spectrum.

of a large number of low-frequency oscillations (see the table), only one-quarter of the CrO_2Cl_2 molecules are in the ground state. When the excitation is by narrow-band laser radiation, a rotational structure can be observed in the electron-vibrational spectrum of the $B_1 \leftarrow A_1$ band.⁷ Therefore in excitation by narrow-band laser radiation the inhomogeneous broadening of the induced absorption band $k_{\text{ind}}(\omega, t = 0)$ may turn out to be smaller than the broadening of the fundamental bands ν_1 and ν_6 , since all the molecules that are distributed at $T = 300\text{ K}$ over the lower vibrational-rotational levels are then involved in the absorption.

Figure 4 shows the induced-clearing band obtained at the instants 0.5 and 1 μsec after the pump pulse when probed by the diode laser. The clearing bandwidth is 9 cm^{-1} (at half-maximum). In the region of the abrupt edge of the Q branch of the ν_6 band, a clearing peak of collision origin appears at a frequency 1002 cm^{-1} . A more detailed structure of this peak is shown in the inset of Fig. 4 together with the corresponding section of the ν_6 -band absorption spectrum.

4. CALCULATION OF INDUCED-ABSORPTION SPECTRUM

At present there is no single approach to the determination of the spectra of molecules with high vibrational-excitation levels. The very cause of the basic change of the spectral properties of molecules in the QC is a moot point.^{12–17} Namely, multimode anharmonicity causes mixing of the closely-lying vibrational states, leading to a redistribution of the strength of the transition of the IR active mode. Thus, a quasicontinuous broadened band is produced instead of individual lines that are resolved in the harmonic approximation. It is this band broadening in the QC which is called homogeneous. We note that the number of experiments on direct probing of the QC is small, and their interpretation is

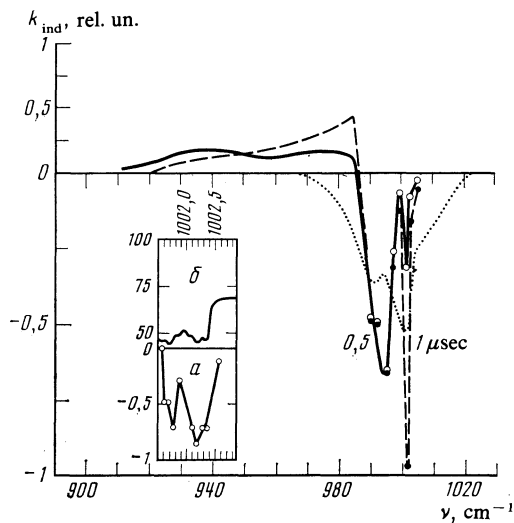


FIG. 4. Dependence of induced clearing on the frequency of semiconductor-laser probing radiation. The solid and dashed curves correspond to probing at the instants 0.5 and 1 μsec after the pump pulse. The energy density of the exciting radiation is 20 mJ/cm^2 , and the pressure in the cell is 0.5 Torr. The dotted curve is the spectrum of the IR radiation of the ν_1 and ν_6 bands of the CrO_2Cl_2 molecule. The inset shows a section of the induced clearing spectrum (a), in relative units, corresponding to the peak at the frequency 1002 cm^{-1} , as well as the corresponding section (b) of the IR transmission spectrum in percent (b), as recorded using the semiconductor laser.

made complicated in most cases by the broad distribution of the populations over the molecule levels. This complication is partially overcome in our procedure. Therefore the "hot-molecule" spectra obtained with short delay can be used to determine directly the QC parameters.

We shall use hereafter the theory developed in Ref. 16 for the calculation of the spectra of excited molecules. Our basic significant assumption is that the hot-molecule excitation level ($\sim 19000 \text{ cm}^{-1}$) is indeed in the QC region. Although for molecules with ≈ 5 atoms the level of the start of the QC is usually estimated as $E_{\text{QC}} < 10^4 \text{ cm}^{-1}$, this assumption must be experimentally verified in each particular case.

We formulate now simplifying model assumptions necessitated not because the calculation is basically difficult, but because the CrO_2Cl_2 molecule excitation parameters are insufficiently well defined.

1) The level population of the excited molecule immediately after the start of the pumping is determined only by the Boltzmann distribution over the lower states and by the inequality of the excitation efficiencies (see Sec. 3). At the present stage we excluded completely the role of the residual inhomogeneous broadening, i.e., the ensemble of the hot molecules was assumed in the model calculation to be strictly monoenergetic. Nor was account taken of the transitions with change of the rotational quantum numbers. It will be shown below that the qualitative form of the spectrum shown in Fig. 3 for small delay can be explained also in this approximation.

2) Two modes, ν_1 and ν_6 , are IR-active in the probing region ($\sim 1000 \text{ cm}^{-1}$). However, the small difference between the CrO_2Cl_2 molecule (C_{2v} symmetry) and a tetrahedron allows us to assume that a larger transition strength

is possessed by the ν_6 (B_1) vibration. (The fully symmetric ν_1 (A_1) vibration is not active in the IR spectrum in the case of a tetrahedron.) Therefore, to simplify the model, we shall henceforth regard the ν_6 band as the only IR-active vibration in the frequency region of interest to us.

Following Ref. 16, we consider the most important problem whose solution should, in our opinion, determine the QC properties in each particular case, viz., that of the intermode resonances in the CrO_2Cl_2 molecule. The importance of this problem is qualitatively obvious. Indeed, the harmonic states that are best intermixed are those close in energy (small intermode-resonance defect) and interact on account of a low-order anharmonicity.

The ν_1 mode participates in two of the symmetry-allowed third-order resonances with a defect less than 100 cm^{-1} . These are $2\nu_8 - \nu_1 \approx 5 \text{ cm}^{-1}$ ($\hat{H}_A \propto \hat{x}_8^2 \hat{x}_1$) and $\nu_1 - 2\nu_2 \approx 45 \text{ cm}^{-1}$ ($\hat{H}_A \propto \hat{x}_2^2 \hat{x}_1$). In none of these does the ν_6 mode take part. Here \hat{H}_A is the anharmonic-interaction operator and \hat{x}_i the coordinate operator of the i th normal vibration. Fourth-order resonances are also more favorable for the ν_1 mode than for ν_6 . We therefore propose for this molecule the following mode-interaction scheme: ν_6 is coupled to ν_1 by a fourth-order anharmonic term

$$\hat{H}_A = V \hat{x}_1^2 \hat{x}_6^2 \quad (3)$$

(V is the anharmonic-interaction constant) with a defect

$$\Delta = 2\nu_6 - 2\nu_1 \approx 14 \text{ cm}^{-1} \quad (4)$$

while the interaction of ν_1 with the other vibrations is strong enough to ensure the proposed stochasticity of this mode.

Under these assumptions, the calculation that follows is based on separating from among all the molecule vibrations the IR-active mode (ν_6 in our case) and regarding all the other degrees of freedom as a reservoir.^{13,15-17} We shall denote the subcontinuum levels without participation of the mode ν_6 , i.e., the reservoir levels, by $|\varepsilon\rangle$. If the interaction (3) is not taken into account, degeneracy exists of the form

$$|v_6=0; \varepsilon=E\rangle, \dots, |v_6=m; \varepsilon=E-m\nu_6\rangle, \dots \quad (5)$$

where v_i are the occupation numbers of the i th modes. v_6 remains here a good quantum number, and the reservoir levels are mixed harmonic states. A change in the structure of the reservoir levels without allowance for (3) does not affect the spectrum, inasmuch as we assume that the transition strength is determined only by the ν_6 mode, i.e., at $V=0$ by the matrix element

$$|\langle v_6=m; \varepsilon | \hat{\mu}(\hat{x}_6) | v_6=m+1; \varepsilon' \rangle|^2 \propto \delta(\varepsilon - \varepsilon'), \quad (6)$$

where $\hat{\mu}$ is the dipole-moment operator.

The subcontinua (5) are related by the interaction (3) which contains the operator \hat{x}_1^2 . By assumption, however, the mode ν_1 is included in the QC of the reservoir levels. By the same token the matrix element (6), as already noted, will be broadened. We introduce a phenomenological broadening constant by defining a "smearing" of the matrix element of the interaction (3). To this end we note first that the matrix elements \hat{H}_A have nonzero values at $\Delta v_6 = 0$ and ± 2 , therefore the degeneracy (5) is not completely lifted. The states mixed have like parity of the quantum number. The correct

states of the vibrational Hamiltonian can be represented in the form.

$$|E\rangle = \sum_{\nu} \sum_{\epsilon} G(E; \epsilon, \nu_6) |v_6, \epsilon\rangle, \quad (7)$$

where the summation includes either even or odd ν_6 . The representation of the correct levels $|E\rangle$ in the form (7) is convenient because the coefficients $G(E; \epsilon, \nu_6)$ are significant at $E \approx \epsilon + \nu_6 \nu_6$. This is proved by the very fact that a pronounced hot-molecule band is observed.

We consider next, by way of example, the matrix elements that connects the level $|v_6, \epsilon\rangle$ with the subcontinuum $|v_6 - 2, \epsilon'\rangle$:

$$\langle \hat{H}_A \rangle = V \langle v_6 - 2 | \hat{x}_6^2 | v_6 \rangle \langle \epsilon' | \hat{x}_1^2 | \epsilon \rangle. \quad (8)$$

Whereas the calculation of the first matrix element of (8) in the harmonic approximation is trivial:

$$\langle v_6 - 2 | \hat{x}_6^2 | v_6 \rangle = v_6^{1/2} (v_6 - 1)^{1/2},$$

additional assumptions must be made concerning the second. If the levels $|\epsilon\rangle$ and $|\epsilon'\rangle$ were to coincide with the harmonic ones, we would have

$$\langle \epsilon' | \hat{x}_1^2 | \epsilon \rangle \propto \delta(\epsilon' - \epsilon \pm 2\nu_1). \quad (9)$$

The assumption that the harmonic states making up the reservoir $|\epsilon\rangle$ are stochastically mixed leads to the conclusion that the matrix element (9) is broadened. It is natural here to assume that the condition (9) determines the center of the contour of the matrix element $\langle \epsilon' | \hat{x}_1^2 | \epsilon \rangle$. As the phenomenological relation we used the Lorentzian

$$|\langle \epsilon' | \hat{x}_1^2 | \epsilon \rangle|^2 = \frac{A}{\pi} \frac{\sigma(\epsilon)}{(\epsilon' - \epsilon - 2\nu_1)^2 + \sigma^2(\epsilon)}. \quad (10)$$

The normalization constant A is determined by the condition that the integral squared interaction be conserved:

$$\int \rho(\epsilon') d\epsilon' |\langle \epsilon' | \hat{x}_1^2 | \epsilon \rangle|^2 = \overline{|\langle x_1^2(\epsilon) \rangle|^2} = \sum_{\nu_1=0}^{\nu_1/\nu_1} (\nu_1 + 1) (\nu_1 + 2) \rho'(\epsilon - \nu_1 \nu_1) / \rho(\epsilon). \quad (11)$$

Here $\rho'(\epsilon)$ is the density of states without allowance for the modes ν_1 and ν_6 , and $\rho(\epsilon)$ is the density of states of the molecule without allowance for ν_6 . Thus,

$$A = \overline{|\langle x_1^2(\epsilon) \rangle|^2} / \rho(\epsilon + 2\nu_1). \quad (12)$$

We have retained in (10) only the term $\epsilon' \approx \epsilon + 2\nu_1$, since the level exactly resonant to $|v_6, \epsilon\rangle$ is $|v_6 - 2, \epsilon + 2\nu_6\rangle$, and $\nu_6 \approx \nu_1$. The interaction with the state $|v_6 + 2, \epsilon''\rangle$ is similarly treated.

The relation between the introduced parameters V and σ can be also estimated by starting from a comparison of the molecule's intermode resonances the determine these quantities. V is a fourth-order-interaction constant, and σ is determined from our assumption concerning the hierarchy of the resonances,¹⁶ mainly third-order resonances. Thus, coordinated variation of the parameters V and σ is possible under the condition

$$V \ll \sigma. \quad (13)$$

The inequality (14) permits explicit determination of the

function $G^2(E; \epsilon, \nu_6)$ from (7). Indeed, knowing the contour of the interaction (10) between the selection level $|v_6, \epsilon\rangle$ and the subcontinua $|v_6 - 2, \epsilon'\rangle$ and $|v_6 + 2, \epsilon''\rangle$ we can determine the manner of broadening of this level.¹⁸ The condition (14) permits this result to be used as a first approximation of the function G^2 . The solution of the problem can be written in the form¹⁸

$$G^2(E; \epsilon, \nu_6) = \frac{1}{\pi} \frac{\delta_1(\lambda) + \delta_2(\lambda)}{[\lambda - d_1(\lambda) - d_2(\lambda)]^2 + [\delta_1(\lambda) + \delta_2(\lambda)]^2}, \quad (14)$$

where

$$\lambda = E - \epsilon - \nu_6 \nu_6, \quad (15)$$

$$\delta_1(\lambda) = V^2 \nu_6 (\nu_6 - 1) \overline{|\langle x_1^2(\epsilon) \rangle|^2} \frac{\sigma(\epsilon)}{(\lambda + \Delta)^2 + \sigma^2(\epsilon)}, \quad (16)$$

$$\delta_2(\lambda) = V^2 (\nu_6 + 2) (\nu_6 + 1) \frac{\rho(\epsilon - 2\nu_1)}{\rho(\epsilon)} \times \overline{|\langle x_1^2(\epsilon - 2\nu_1) \rangle|^2} \frac{\sigma(\epsilon - 2\nu_1)}{(\lambda - \Delta)^2 + \sigma^2(\epsilon - 2\nu_1)}, \quad (17)$$

$$d_1(\lambda) = V^2 \nu_6 (\nu_6 - 1) \overline{|\langle x_1^2(\epsilon) \rangle|^2} \frac{\lambda + \Delta}{(\lambda + \Delta)^2 + \sigma^2(\epsilon)}, \quad (18)$$

$$d_2(\lambda) = V^2 (\nu_6 + 2) (\nu_6 + 1) \frac{\rho(\epsilon - 2\nu_1)}{\rho(\epsilon)} \times \overline{|\langle x_1^2(\epsilon - 2\nu_1) \rangle|^2} \frac{\lambda - \Delta}{(\lambda - \Delta)^2 + \sigma^2(\epsilon - 2\nu_1)}. \quad (19)$$

The function $G^2(\lambda)$ is normalized by the condition

$$\int_{-\infty}^{+\infty} G^2(\lambda) d\lambda = 1. \quad (20)$$

When the condition (13) is satisfied, the resultant function (14) has a dispersion shape with a maximum at $E \approx \epsilon + \nu_6 \nu_6$ and an effective half-width $\approx \delta_1(0) + \delta_2(0)$. The deviation of (14) from a Lorentzian shape is manifest in the tail ($\lambda \gg \delta_1(0) + \delta_2(0)$), where $G_2(\lambda) \propto 1/\lambda^4$.

Knowing the coefficients of the expansion of $G_2(E; \epsilon, \nu_6)$ we can determine also the absorption spectrum, i.e., the matrix element $|\langle E | \hat{\mu} | E' \rangle|^2$, where $E' = E + \nu_{\text{prob}}$:

$$|\langle E | \hat{\mu} | E' \rangle|^2 \propto \sum_{\nu_6} (\nu_6 + 1) \int d\epsilon G^2(E; \epsilon, \nu_6) \times G^2(E'; \epsilon, \nu_6 + 1) \rho(E - \nu_6 \nu_6). \quad (21)$$

The integration in (21) is elementary, and the lengthy final results will not be given here.

So far we did not mention the regular shift of the absorption spectrum, which is determined by the average scalar-anharmonicity constant (see, e.g., Ref. 16):

$$\nu(E) = \nu_0 - X_0(E/\nu_6), \quad (22)$$

$$X_0 = \frac{1}{N} \sum X_{6i\nu_6} (1 + \delta_{i6}) \frac{g_i}{\nu_i}.$$

Here N is the number of vibrational degrees of freedom ($N = 9$ for CrO_2Cl_2). The summation is over the normal modes, g_i is their degeneracy. X_{6i} are the intermode-anharmonicity constants, and δ_{i6} is the Kronecker delta. Separation

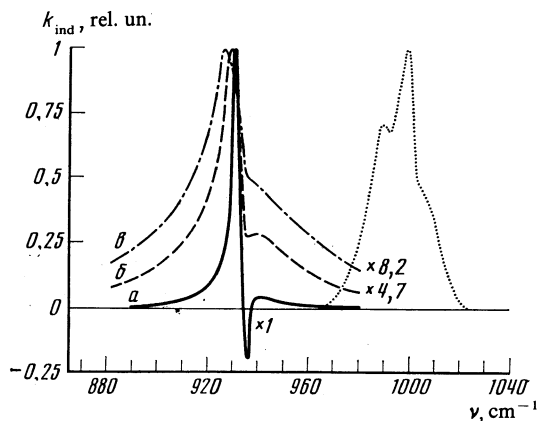


FIG. 5. Calculated induced-absorption spectrum obtained at different relations between the parameters ($\sigma(\epsilon) = \text{const} = 30 \text{ cm}^{-1}$, $X_0 = 3.7 \text{ cm}^{-1}$): a— $V = 0.75 \text{ cm}^{-1}$; b— $V = 1.5 \text{ cm}^{-1}$; c— $V = 2 \text{ cm}^{-1}$. The dotted curve shows the absorption spectrum corresponding to the modes ν_1 and ν_6 .

tion of the cold- and hot-molecule bands in the spectrum makes it easy to estimate the constant X_0 :

$$X_0 \approx \frac{\nu_{\text{cold}}^{\text{max}} - \nu_{\text{hot}}^{\text{max}}}{\bar{E}_{\text{hot}} - \bar{E}_{\text{cold}}} \nu_6. \quad (23)$$

The induced-emission contour calculated in analogy with (14) is thus shifted towards shorter wavelengths and has a maximum at the frequency $\nu(E) + X_0$.

Before presenting the calculation results, we call attention to the difference between the model considered here and that of Ref. 16. In principle, the best model parameters would be the averaged anharmonic-interaction constants. The broadenings observed in the spectrum and their evolution with increasing energy would then be determined by these constants and by the increase of the interaction matrix elements with energy. This was precisely the procedure in Ref. 16. The same constants determine also the introduced broadening σ . Since, however, the experimental spectrum was obtained at only one pump frequency, it is meaningless to vary parameters that can be determined only by comparing the calculations with the spectra for different hot-molecule energies. For our purposes it is therefore equally correct to use the quantity σ as the varied parameter.

Another feature is that participating in our model is

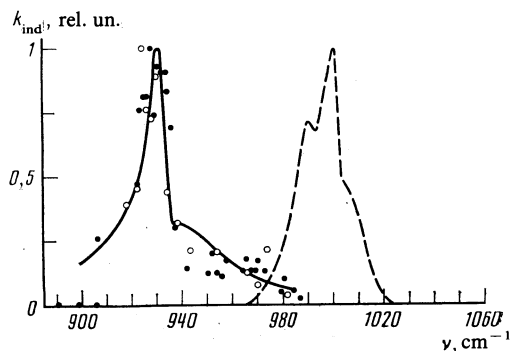


FIG. 6. Comparison of calculated and experimental induced-absorption spectra; the calculation was performed with the parameters (24). Dashed line—absorption spectrum corresponding to the modes ν_1 and ν_6 .

only one resonance that relates ν_6 to the reservoir of the other degrees of freedom. In Ref. 16 the case of overlapping resonances was considered. The ensuring changes in the calculation of the spectrum do not introduce significant complications since we have restricted, from physical considerations, the relations between the parameters by the inequality (13).

Figure 3 shows by way of illustration the spectra obtained at different relations between V and σ . It is seen from this that the qualitative distinguishing features of the hot-molecule band are determined by the conditions of the up- and down-transitions in the presence of an anharmonic shift. For reconciliation with experiment (Fig. 6), we used the parameters

$$V = 1.5 \text{ cm}^{-1}, X_0 = 3.7 \text{ cm}^{-1}, \quad (24)$$

$$\sigma(\epsilon) = 30 \text{ cm}^{-1} - 1.5 \cdot 10^{-3} (E - \epsilon).$$

Note that out of the three parameters in (24) and X_0 is determined with sufficient accuracy, while V and σ give only the order of magnitude. They can be determined more accurately by comparing the calculations with experiment at a different pump frequency (see the Conclusion).

For the matrix element $\langle \epsilon' | \hat{x}_1^2 | \epsilon \rangle$ [i.e., $\sigma(\epsilon)$] the functional dependence of the broadening is not so important. The point is that the principal role is absorption and emission are played by subcontinua with small ν_6 . The average occupation number ν_6 can be estimated at $\bar{\nu}_6 \approx E_0 / N \nu_6 \approx 2$. In particular, taking into account the increase of the matrix element $\langle \nu_6 | \hat{\mu} | \nu_6 \pm 1 \rangle^2$, the main contribution to (23) (80% in terms of the integral) is made by states with $\nu_6 = 0-5$.

5. VIBRATIONAL RELAXATION OF HIGHLY EXCITED CrO_2Cl_2 MOLECULES

Under the conditions of our experiment a pump pulse transfer approximately 1.5% of the CrO_2Cl_2 molecules into a state with energy $\approx 1.9 \cdot 10^4 \text{ cm}^{-1}$. In collisions with unexcited molecules, a transition to a Boltzmann distribution takes place in the hot ensemble. At the same time, the average energy of the hot ensemble is lowered by energy transfer to other initially cold molecules. Figure 7 shows the dependence of the average excitation level of the hot molecule ensemble on the time elapsed after the pump pulse. This dependence was obtained from the induced-absorption spectra for different delay times (see Fig. 3). Such spectra allow us to track the evolution of the distribution function and determine the relaxation rate constants.

A detailed theory of the relaxation of vibrationally

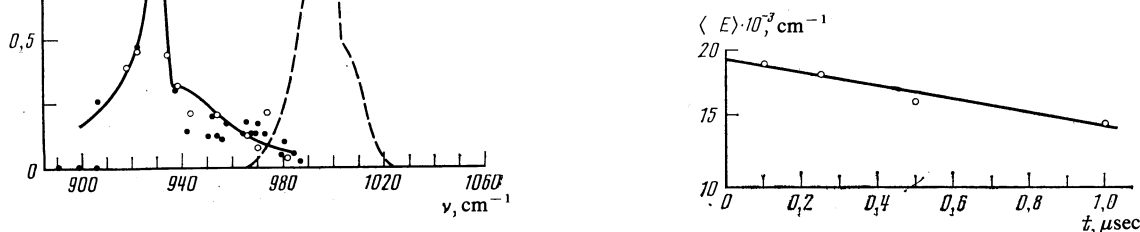


FIG. 7. Time dependence of average excitation level of CrO_2Cl_2 molecules. The pressure of the CrO_2Cl_2 gas in the cell is 0.5 Torr.

highly excited molecules from an initially narrow distribution is expounded in Ref. 19. The time evolution of the spectra (Fig. 3) is in full agreement with that theory, viz., the spectra broaden and shift towards shorter wavelengths. This change of the spectra corresponds to diffusion and drift over the QC vibrational levels. The time dependence of the average energy is given by¹⁹

$$E(t) = E_0 \left\{ \frac{1}{a} \exp \left[-\frac{a \langle \Delta E(E_0) \rangle}{E_0} Zt \right] - \frac{1-a}{a} \right\}, \quad (25)$$

where E_0 is the maximum excitation energy, Z is the frequency of the gaskinetic collisions, and a is a parameter ($0 \leq a \leq 1$) that determines the dependence of the average energy transfer per collision of the excitation energy:

$$\langle \Delta E(E) \rangle = \langle \Delta E(E_0) \rangle (1 - a + aE/E_0). \quad (26)$$

Comparing the experimental dependence (Fig. 7) with the theoretical (25) we can obtain the average transfer per collision:

$$\begin{aligned} \langle \Delta E(E_0) \rangle &= 1300 \pm 200 \text{ cm}^{-1}, \quad a=1. \\ \langle \Delta E(E_0) \rangle &= 1100 \pm 200 \text{ cm}^{-1}, \quad a=0. \end{aligned} \quad (27)$$

The collision cross section for the CrO_2Cl_2 molecule was chosen in accord with the hard-sphere approximation, so that the collision frequency was $Z = 8.2 \cdot 10^6 \text{ sec}^{-1}$ at a CrO_2Cl_2 gas pressure 1 Torr. The experimental accuracy and the short analyzed time interval ($0.1\text{--}1 \mu\text{sec}$) do not permit a determination of the parameter a .

Laser excitation followed by internal conversion into the ground electronic state was successfully used to study vibrational relaxation in Refs. 20–23. The probing in this case was by the methods of UV absorption^{20,21} and IR fluorescence.^{22,23} It was found in Ref. 23 that when azulene molecules were excited to energy levels $E_0 = 17500$ and 30600 cm^{-1} the average energies consumed in collisions between the azulene molecules were 1217 ± 48 and $1425 \pm 31 \text{ cm}^{-1}$ respectively. For toluene molecules readied in the state $E_0 = 52000 \text{ cm}^{-1}$ the result was $\langle \Delta E(E_0) \rangle = 770 \pm 150 \text{ cm}^{-1}$ at $a < 0.25$ (Ref. 20).

6. CONCLUSION

In the present study we have demonstrated, with the CrO_2Cl_2 molecule as an example, the capabilities of a new method for spectroscopy of highly excited vibrational levels in the electronic ground state. In that part of the experiment devoted to the manner of readying the molecules in the excited states, the method is not universal. It is applicable only to molecules that have electronic states located at least below the dissociation limit. For such molecules, however, the method is quite simple and yields interesting information on the spectra of transitions from highly excited vibrational states. We note that IR absorption spectroscopy is not the only method for probing molecules excited in this manner. Other methods are possible in conjunction with excitation via a nonradiative transition, viz., IR fluorescence, spontaneous Raman scattering, and coherent active Raman-scattering spectroscopy.

Our aim here is not to discuss the relative advantages and shortcomings of these methods in the study of spectra of

highly excited vibrational states. We note only that it is precisely the combination of IR probing with probing by Raman scattering which is capable of yielding the most complete information on the properties of the spectra of practically all vibrational bands of the investigated molecule. In our opinion, the most interesting feature of the spectra of vibrational transitions from highly excited states is the homogeneous broadening. As follows from the theoretical analysis in Ref. 16, this quantity, generally speaking, is different for different bands, and the more complete the set of experimental results the more complete the information that can be extracted from them on the intermode interactions in the molecule.

The theoretical analysis of Sec. 4 is illustrative only, and cannot claim completeness. The main reason is that we do not know the inhomogeneous spectral-broadening component due to the spread of the energies of the molecules readied in highly excited states. However, the experimental fact that the width of the clearing contour in the spectrum of the molecules that remain in lower vibrational levels is smaller than the width of the absorption contour for the excited molecules indicates that the model and the intermode-interaction parameters calculated in it are realistic. Another shortcoming of the calculation is failure to take into account the rotational structure of the transition. It is difficult to overcome this shortcoming, since we do not know the rotational states with which the second harmonic of an Nd:YAG laser interacts predominantly. In addition, as noted in Sec. 4, the fit of the calculation results to the experiment is not fully single-valued. The ambiguity can be eliminated by varying the molecule excitation energy.

All the foregoing indicates the best direction for further progress. To obtain experimental results that can be more accurately interpreted the gas must be cooled (say, in a supersonic jet) and the molecules should be excited with a tunable laser of sufficient power. The spectrum width obtained in such an experiment will decide ultimately whether the investigated excitation energy lies in the region of the vibrational continuum or, which is the same,¹ in the stochasticity region of the vibrational motion. In this paper we have assumed without proof (see the Title) that this is the case, and the calculation was performed just under this natural assumption, even though the lower limit of the stochasticity region for CrO_2Cl_2 is unknown. Furthermore, this limit could be experimentally estimated for only two examples, SF_6 and CF_3I (Ref. 24), namely $3900 \pm 500 \text{ cm}^{-1}$ for SF_6 and $6000 \pm 500 \text{ cm}^{-1}$ for CF_3I .

At present there is only one method that is an alternative of ours for the spectroscopy of a vibrational continuum of polyatomic molecules. This is ordinary linear absorption spectroscopy of high-frequency vibrational modes (e.g., of C–H vibrations). In addition to Refs. 2–5 cited in the Introduction, where the spectra of high overtones were investigated, we point out also Refs. 15 and 16, where the spectra of the fundamental bands of C–H vibrations and of their first overtones were investigated in the molecules $(\text{CF}_3)_3\text{CH}$ and $(\text{CF}_3)_3\text{C} - \text{C} \equiv \text{C} - \text{H}$. However, linear spectroscopy is suitable for the study of a vibrational quasicontinuum only in the case of high-frequency vibrations and (or) very com-

plex molecules with a low low-lying quasicontinuum boundary; its capabilities are furthermore limited by the attainable vibrational energy. This is why it is of interest to search for universal methods that can make ready molecules in highly excited vibrational energies with an narrow an energy distribution as possible. Such methods are: 1) direct pumping of a high overtone; 2) biharmonic pumping; 3) resonant excitation by a strong IR field under conditions when the energy-distribution width is satisfactorily small; 4) resonant collisional energy transfer from laser-excited atoms.

The authors thank V. S. Letokhov, V. G. Koloshnikov, Yu. G. Vainer, and M. R. Aliev for helpful discussions, as well as I. I. Zasavitskiĭ and A. P. Shotov for supplying the diode lasers.

¹V. N. Bagratashvili, V. S. Letokhov, A. A. Makarov, and E. A. Ryabov, *Laser Chem.* **1**, 211 (1983). V. N. Bagratashvili, V. S. Letokhov, A. A. Makarov, and E. A. Ryabov, *Multiphoton Processes in Molecules in an IR Laser field*, VINITI, ser. Fizika atoma i molekuly (Atom and Molecule Physics), Vol. 1, 1981.

²G. J. Scherer, K. K. Lehmann, and W. Klemperer, *J. Chem. Phys.* **78**, 2817 (1983).

³R. A. Bernheim, F. W. Lampe, J. F. O'Keefe, and J. R. Hill III, *Chem. Phys. Lett.* **100**, 45 (1983).

⁴K. V. Reddy, D. F. Heller, and M. J. Berry, *J. Chem. Phys.* **76**, 2814 (1982).

⁵G. A. West, R. P. Maretta Jr., J. E. Pete, *et al.*, *ibid.* **75**, 2006 (1981).

⁶J. R. McDonald, *Chem. Phys.* **9**, 423 (1975).

⁷J. A. Blaxy and D. H. Levy, *J. Chem. Phys.* **69**, 2901 (1978).

⁸R. N. Dizon and C. R. Webster, *J. Mol. Spectrosc.* **62**, 271 (1976).

⁹W. E. Hobbs, *J. Chem. Phys.* **28**, 1220 (1958).

¹⁰H. Stammerich, K. Kawai, and Y. Taveres, *Spectrochim. Acta* **9**, 438 (1959).

¹¹F. A. Miller, G. L. Carlson, and W. B. White, *ibid.* **9**, 709 (1959).

¹²A. A. Makarov, in: *Use of Lasers in Atomic, Molecular, and Nuclear Spectroscopy*, Proc. 2nd All-Union School [in Russian], Nauka, 1983, p. 67.

¹³K. G. Kay, *J. Chem. Phys.* **75**, 1690 (1982).

¹⁴J. Stone, E. Thiele, and M. F. Goodman, *ibid.*, p. 1712.

¹⁵I. Shek and J. Jortner, *ibid.* **70**, 3016 (1979).

¹⁶A. A. Makarov and V. V. Tyakht, *Zh. Eksp. Teor. Fiz.* **83**, 502 (1982) [*Sov. Phys. JETP* **56**, 274 (1982)].

¹⁷D. P. Hodgkinson and J. S. Briggs, *Chem. Phys. Lett.* **43**, 451 (1976).

¹⁸A. A. Makarov, V. T. Platonenko, and V. V. Tyakht, *Zh. Eksp. Teor. Fiz.* **75**, 2075 (1978) [*Sov. Phys. JETP* **48**, 1044 (1978)].

¹⁹J. Troe, *J. Chem. Phys.* **77**, 3485 (1982).

²⁰H. Hippler, J. Troe, and H. J. Wendelken, *ibid.* **78**, 6709 (1983).

²¹H. Hippler, J. Troe, and H. J. Wendelken, *ibid.* p. 6718.

²²G. P. Smith and J. R. Barker, *Chem. Phys. Lett.* **78**, 253 (1981).

²³M. J. Rossi, J. R. Pladziewicz, and J. R. Barker, *J. Chem. Phys.* **78**, 6695 (1983).

²⁴V. N. Bagratashvili, Yu. G. Vainer, V. S. Dolzhkov, *et al.*, *Zh. Eksp. Teor. Fiz.* **80**, 1008 (1981) [*Sov. Phys. JETP* **53**, 512 (1981)].

²⁵H. R. Dübal and M. Quack, *Chem. Phys. Lett.* **72**, 342 (1980).

²⁶K. von Putheamer, H. R. Dübal, and M. Quack, *ibid.* **95**, 358 (1983).

Translated by J. G. Adashko